Geosci. Model Dev. Discuss., 6, 1467–1494, 2013
www.geosci-model-dev-discuss.net/6/1467/2013/
doi:10.5194/gmdd-6-1467-2013

Geoscientific Model Development Discussions
Open Access

δ^{18}O water isotope in the *i*LOVECLIM model (version 1.0) – Part 1: Implementation and verification

D. M. Roche[1,2]

[1]Earth and Climate Cluster, Faculty of Earth and Life Sciences, Vrije Universiteit Amsterdam, Amsterdam, the Netherlands
[2]Laboratoire des Sciences du Climat et de l'Environnement (LSCE), UMR8212, CEA/CNRS-INSU/UVSQ, Gif-sur-Yvette Cedex, France

Received: 5 February 2013 – Accepted: 18 February 2013 – Published: 4 March 2013

Correspondence to: D. M. Roche (didier.roche@vu.nl)

Published by Copernicus Publications on behalf of the European Geosciences Union.

Abstract

A new ^{18}O stable water isotope scheme is developed for three components of the *i*LOVECLIM coupled climate model: atmospheric, oceanic and land surface. The equations required to reproduce the fractionation of stable water isotopes in the simplified atmospheric model ECBilt are developed consistently with the moisture scheme. Simplifications in the processes are made to account for the simplified vertical structure including only one moist layer. Implementation of these equations together with a passive tracer scheme for the ocean and a equilibrium fractionation scheme for the land surface leads to the closure of the (isotopic-)water budget in our climate system. Following the implementation, verification of the existence of usual δ^{18}O to climatic relationships are performed for the Rayleigh distillation, the Dansgaard relationship and the δ^{18}O–salinity relationship. Advantages and caveats of the approach taken are outlined.

1 Introduction

Water isotopes are widely used tracers of the hydrological cycle. With fractionation occuring at phase changes (evaporation, condensation, freezing, e.g. Craig and Gordon, 1965) and through diffusive processes at smaller scale, water isotopes are faithful recorder of the complex processes at work within the hydrological cycle. They have been used for decades in the field of paleoclimate research to infer climatic conditions from the ice-cores (Dansgaard, 1964; Dansgaard et al., 1993; EPICA community members, 2004; North Greenland Ice Core Project members, 2004) or from oceanic sediment cores (Emiliani, 1955, for example) but may also be used at much smaller time and spatial scale to link climate variability and water isotopes composition (Kurita et al., 2011) or even to infer the mixing properties within rain events (Risi et al., 2010a).

From a climatic modelling perspective, the inclusion of water isotopes enable a thorough evaluation of the hydrological cycle in climate models, not only against precipitation amount or evaporation amount observations, but also on the actual transport of water through the atmospheric model. Applied to paleoclimate simulations, it enables an accurate comparison of the model results with paleoproxies, avoiding intermediate steps through derivation of temperature or salinities. Finally, it is an important procedure to assess the closure and adequate transport of water within models since any non-conserving process will likely lead to unrealistic δ^{18}O of water. Since the pioneering work of Joussaume et al. (1984), much progress has been achieved in Atmospheric General Circulation models (Hoffmann et al., 1998; Noone and Simmonds, 2002; Mathieu et al., 2002; Tindall et al., 2009, for example) that can simulate quite accurately the δ^{18}O of precipitation, even at fine resolution (Werner et al., 2011). Some secondary parameters like the deuterium excess have proven to be more challenging (Risi et al., 2010). The development of water isotope enabled isotopic models (Schmidt, 1998; Delaygue et al., 2000, for example) have further enabled the use of coupled isotope enabled climate models that are then applied to paleoclimate science questions (Legrande and Schmidt, 2008, for example).

Given the computing ressources needed to run coupled climate models, applying less complex coupled climate models with water isotopes to long term paleoclimate perspectives is still promising. The requirement, given the nature of isotope fractionation and distillation processes within the atmosphere (Craig and Gordon, 1965), is to explicitly compute the transport of water isotopes within the atmosphere. Early attempts (Roche et al., 2004, for example) have shown that such a perspective, though clearly not applicable for kilometer scale issues, could help towards a better understanding of paleoproxy records. This is the approach taken in the present study that comprises three parts: (1) development and verification, (2) evaluation against water isotopes observations, (3) evaluation against carbonate isotopes proxy data.

In the present manuscript, I present the design and verification of a δ^{18}O water isotopes module in the *i*LOVECLIM climate model. I start with the equations needed to simulate the water isotopes in our simplified coupled climate model and proceed to the verification against well-known relationships of the climate system. In the two companion manuscripts, we present the model validation and evaluation, at first from the perspective of δ^{18}O in water from present-day observations (Roche and Caley, 2013) and second with a paleo-perspective against Late Holocene carbonate proxy data (Caley and Roche, 2013).

2 Technical description of the water isotopic scheme used in *i*LOVECLIM

The *i*LOVECLIM model is a code fork of the LOVECLIM-1.2 climate model extensively described in Goosse et al. (2010). From the original model, we retain the atmospheric (ECBilt), oceanic (CLIO), vegetation (VECODE) and land-surface (LBM) components and developed a complete, conservative, water isotope cycle through all cited components. With regards to water isotopes, the main development lies in the atmospheric component in which evaporation, condensation and existence of different phases (liquid and solid) all affect the isotopic conditions of the water isotopes. Hence, I first describe extensively in the following the method used to trace the water isotopes in ECBilt and only briefly their treatment in other components afterwards.

2.1 ECBilt-wiso: water isotopes tracking in the atmosphere

ECBilt is the simplified component of the *i*LOVECLIM Earth System Model. It is a quasi-geostrophic atmospheric model with some additional correction terms, described in details in Opsteegh et al. (1998) and Goosse et al. (2010). The atmosphere runs at a T21L3 resolution, that is approximatedly 5.6° resolution in latitude and longitude. Of main interest for the purpose of developing a water isotopic module is the water cycle dynamics. ECBilt contains a full description of the water cycle from the evaporation to precipitation through condensation. The vertical structure is on three levels with only one humid layer (troposphere) and two dry layers (stratosphere). A schematic representation of the water cycle in ECBilt is given in Fig. 1. Evaporative water fluxes are added to the humid layer. Then vertical advection is computed. Since the two upper layers are dry, water fluxes crossing the boundary between the troposphere and the stratosphere is rained out as convective rain. If the water specific humidity of the humid layer is greater than a specific q_{sat} value (set in ECBilt as 80 % of the saturation humidity at given temperature), the excess water is removed as large scale precipitation. Finally, if large scale precipitation occurs with negative temperatures, excess precipitation is removed as large scale snowfall.

2.1.1 Prognostic variable for water isotopes

For water isotopes, I follow roughly the same procedure. The prognostic variable for humidity in ECBilt is the quantity of precipitable water for the whole atmospheric column, $\tilde{q}$. It may be written as:

$$\tilde{q} = \frac{m_{\mathrm{H_2O}}}{S\ \rho} = \frac{nM_{\mathrm{H_2O}}}{S\ \rho} \tag{1}$$

where $m_{\mathrm{H_2O}}$ is the mass of water in the given cell S the surface of the cell, ρ the water density, n the number of moles of water and $M_{\mathrm{H_2O}}$ the molar mass.

The water isotope variable to be used is, by analogy, written here for ^{18}O:

$$\tilde{q}^{18} = \frac{n^{18} M^{18}_{\mathrm{H_2O}}}{S\ \rho} \tag{2}$$

However, since the interaction of the different water isotopic species that form the water will not be dealt with, the previous formulation may be simplified to have the water isotopes as a simple tracer of water as in Merlivat and Jouzel (1979). Thus, the water isotopic quantity is expressed as:

$$\tilde{q}^{18} = R^{18}\tilde{q} \tag{3}$$

Let us now describe the isotopic changes throughout the water cycle, from evaporation to precipitation.

2.1.2 Isotopic evaporation

At the evaporation stage, the formulation for water is $E = \Pi(q_\mathrm{s} - q_\mathrm{v})$ where q_s is the surface specific humidity above the ocean and q_v the humidity of the first layer above the ocean. For the water isotopes, the equivalent formulation is:

$$E^i = \Pi^{18}\left(q_\mathrm{s}^{18} - q_\mathrm{v}^{18}\right) \tag{4}$$

where the ^{18} denote the oxygen-18 related terms. To simulate the water isotopes in the evaporation, we need to determine q_s^{18}. However, in ECbilt, the terms q_s and q_v are computed from a climatological discretisation on the vertical to take into account the effect of the planetary boundary layer. Since there is no equivalent vertical discretisation for water isotopes, I cannot use the same procedure and need to rely on an approximate solution, computing first the water isotopic ratio in the evaporation. That obtained and using the property that, with the given definitions, we can write:

$$R_E^i = \frac{E^{18}}{E} \tag{5}$$

the computation of E^{18} follows logically. Computing R_E^{18} requires some assumption on the processes occuring between the ocean and the atmosphere. I chose here to use the method introduced by Cappa et al. (2003) with a slight modification to account for our context.

Cappa et al. (2003) assume that at the interface of the ocean, there is a thin layer in equilibrium with the ocean, overlaid by the planetary boundary layer that exchange moisture with the free atmosphere and the previous thin equilibriated layer. I will not repeat the equations developed by these authors here since they apply to our case and only repeat the resulting final formulation for R_E^{18}:

$$R_E^{18} = \alpha^*_\mathrm{diff}\frac{R_\mathrm{eq}^{18} - h_\mathrm{a}R_\mathrm{a}^{18}}{1 - h_\mathrm{a}} \tag{6}$$

where h_a is the relative humidity and R^{18}_a the isotopic ratio in the free atmosphere, R^{18}_eq is the isotopic ratio at equilibrium with the ocean and α^*_diff is the kinetic fractionation factor for the isotope considered. To obtain the previous formulation, Cappa et al. (2003) assume implicitly that the saturated humidity is the same at the ocean surface and in the free atmosphere. This is not the case for the ECBilt model. I thus need to modifiy slightly the previous equation, introducing the saturated specific humidity in both the free atmosphere and in the thin equilibrated layer above the ocean. An "apparent" relative humidity for the free atmosphere may be defined as:

$$h^*_\mathrm{a} = h_\mathrm{a}\frac{q_{\mathrm{eq}_\mathrm{a}}}{q_{\mathrm{eq}_\mathrm{s}}} \tag{7}$$

where h_a is the model free atmosphere relative humidity, $q_{\mathrm{eq}_\mathrm{a}}$ the specific free atmosphere humidity and $q_{\mathrm{eq}_\mathrm{s}}$ the specific humidity of the equilibrated thin layer above the ocean. Using the apparent relative humidity, Eq. (6) can finally be used to compute the isotopic ratio of evaporating moisture as:

$$R^{18}_E = \alpha^*_\mathrm{diff}\frac{R^{18}_\mathrm{eq} - h^*_\mathrm{a}R^{18}_\mathrm{a}}{1 - h^*_\mathrm{a}} \tag{8}$$

where:

$$\alpha^*_\mathrm{diff} = \frac{\Pi^{18}}{\Pi} = \left[\frac{D^{18}}{D}\right]^n \tag{9}$$

The $\frac{D^{18}}{D}$ coefficient is determined experimentally. In *i*LOVECLIM, the values determined by Merlivat (1978) for ^{18}O are used, that is:

$$\frac{D^{18}}{D^{16}} = 0.9723 \tag{10}$$

which fully determine the isotopic evaporation in our model.

2.1.3 Water isotopes in precipitation

As described previously, we have only one moist level and only two types of precipitation. A full description of the fractionation for precipitation would need to describe the processes from the distillation between the liquid droplets formation and atmospheric moisture to the re-equilibration of falling precipitation with its surrounding moist air. Since the ECBilt model does not allow such an implementation, I rely on a very simple approach. I assume that precipitation always forms in isotopic equilibrium with the surrounding moisture with instantaneous rainout to the surface. For convective liquid precipitation, I use the equilibrium isotopic ratios at the altitude of the tropopause whereas for large scale liquid precipitation, I use the mid-troposphere conditions. In the case of solid precipitation (snow), I consider it to be always in equilibrium with isotopic moisture at the tropopause. However, to account for enhanced kinetic fractionation that was reported in high latitude regions, the formula of Merlivat and Jouzel (1979) is used. Thus our scheme may be summarized as:

$$R^{18}_{\text{lsp}} = \alpha^{18}_{\text{l-v}}\left(T_{\text{Tropo}}\right) R^{18}_{\text{v}} \tag{11}$$

$$R^{18}_{\text{cp}} = \alpha^{18}_{\text{l-v}}\left(T_{\text{Strato}}\right) R^{18}_{\text{v}} \tag{12}$$

$$R^{18}_{\text{sn}} = {}^{\text{kin}}\alpha^{18}_{\text{s-v}}\left(T_{\text{Strato}}\right) R^{18}_{\text{v}} \tag{13}$$

where $\alpha^{18}_{\text{l-v}}$ is taken from Majoube (1971b) as:

$$\alpha^{18}_{\text{l-v}}(T) = \exp\left(\frac{1137}{T^2} - \frac{0.4156}{T} - 0.0020667\right) \tag{14}$$

and ${}^{\text{kin}}\alpha^{18}_{\text{s-v}}$ derives from $\alpha^{18}_{\text{s-v}}$ as in Merlivat and Jouzel (1979):

$${}^{\text{kin}}\alpha^{18}_{\text{s-v}} = \frac{\alpha^{18}_{\text{s-v}} \cdot S}{1 + \alpha^{18}_{\text{s-v}}(S-1)\frac{D}{D^{18}}} \tag{15}$$

where S is a function depending on temperature as:

$$S = 1 - \lambda T \tag{16}$$

and λ is a tunable parameter generally taken between 2×10^{-3} and 4×10^{-3}.

The equilibrium fractionation coefficient between water vapor and solid water is taken from Majoube (1971a) as:

$$\alpha^{18}_{\text{s-v}} = \exp\left(\frac{11.839}{T} - 0.028244\right) \tag{17}$$

which entirely determines our system of equations.

2.2 Water isotopes in other components

In the other components of the earth system, I assume to a first order approximation that the water isotopes act as passive tracers in the ocean and under equilibrium fractionation for the other components.

2.2.1 Land surface model

As precipitation falls on land surface, the water and water isotopes are added to the bucket water model. If re-evaporation occurs, it is assumed to be formed under isotopic equilibrium with environmental conditions. Thus the ratio of oxygen-18 isotopes in re-evaporation is:

$$R^{18}_{\text{reevap}} = \frac{R^{18}_{\text{landsurf}}}{\alpha^{18}_{\text{l-v}}(T)} \tag{18}$$

where T is the local surface temperature. If the amount of (isotopic) water in the soil bucket exceeds a threshold then water is routed instantaneously to the ocean following

Title Page
Abstract | Introduction
Conclusions | References
Tables | Figures
◀| |▶
◀ ▶
Back | Close
Full Screen / Esc
Printer-friendly Version
Interactive Discussion

a simple routing scheme with pre-defined river basins. There is no fractionation associated with that process since there is no phase changes. Similarly, evapotranspiration occurs with equilibrium fractionation from the soil bucket water. Departing from this hypothesis would require to model what is occuring for leaf water: from the bucket water uptake in roots to the transpiration in leafs. This is clearly beyond the modelling scale we are attempting here. Further evolution of the model will test the necessity to use a simplified parametrization going beyond the presented simplistic assumption.

Finally, the snow layer is also represented as a bucket-type: snow piles up until a threshold is reached. When additional snow is added, the snow is routed directly in the ocean following the same routing as for liquid water. As I do not deal with the accumulation of snow in different layers through the course of winter, the snow layer is assumed to be one well mixed layer: additional snow precipitation modifies the δ^{18}O content of all the layer. In turn, snow sublimation produces moisture with δ^{18}O at the snow δ^{18}O, that is the evaporated snow is assumed to be isolated from the rest of the snow layer, as is expected.

2.2.2 Ocean model

Water isotopes are passive tracers in the ocean. Since CLIO is a free surface Oceanic General Circulation Model, I took care to implement the isotopes so as to be mass conserving, following exactly what is done for salinity. This is especially important if one wants to conserve the water isotopes to salinity relationship. In the present initial version, it is assumed that there is no isotopic effect in relationship with sea-ice. The actual measured frationnation is relatively small (on the order of 2 ‰ (Craig and Gordon, 1965; Melling and Moore, 1995) w.r.t. the surface ocean) in comparison with the salinity effect. Since there might be a local effect in regions where sea-ice is formed we plan to implement it in a later version. However, the current state of the sea-ice model dos not allow to easily trace the water isotopic content and overcoming this limitation would need relatively extensive model development.

2.3 Simulation setup

In the following, I present results of a 5000 yr equilibrium run under fixed pre-industrial boundary conditions. The atmospheric pCO_2 is chosen to be 280 ppm, methane concentration is 760 ppb and nitrous oxide concentration is 270 ppb The orbital configuration is calculated from Berger (1978) with constant year 1950. The run is performed using present-day land-sea mask, freshwater routing and interactive vegetation.

With regards to the water isotopes, the atmospheric moisture is initialized at −12 ‰ and the ocean at 0 ‰ for δ^{18}O.

3 Verification: atmospheric component

In order to assess whether the implementation of all the above fractionation factors was successful, we now conduct a verification step for the atmosphere by checking if the model is able to reproduce the expected relationships between simulated δ^{18}O and simulated selected climatological variables.

3.1 Rayleigh distillation

One of the simplest transformations that may occur is the so-called Rayleigh distillation. It is described as follow: starting from a moist air mass with a certain composition ${}^{0}R_{\mathrm{v}}^{18}$, the air mass progressively looses its water by equilibrium precipitation and immediate removal from the air mass. The air mass is assumed to be isolated through this process. Such a process allows to simply relate the humidity of the air mass at a certain point in the drying process to its δ^{18}O composition – or the equilibrium δ^{18}O composition of the next precipitation to be formed.

3.1.1 Theoritical formulation

From a moist air mass of composition ${}^{0}R_{\mathrm{v}}^{18}$ initially:

$$ {}^{0}R_{\mathrm{v}}^{18} = \frac{{}^{0}n_{\mathrm{v}}^{18}}{{}^{0}n_{\mathrm{v}}^{16}} \simeq \frac{{}^{0}n^{18}}{{}^{0}n_{\mathrm{v}}^{w}} \tag{19} $$

where the ${}^{0}n^{i}$ are the different initial molar abundances of ^{18}O,^{16}O and water respectively. Assuming that the first condensation process modifies the ratio of the δ^{18}O of the moist air mass by $\mathrm{d}R_{\mathrm{v}}^{18}$, we may write:

$$ \mathrm{d}R_{\mathrm{v}}^{18} = \mathrm{d}\left(\frac{n_{\mathrm{v}}^{18}}{n_{\mathrm{v}}^{w}}\right) = \frac{\mathrm{d}n_{\mathrm{v}}^{18}}{n_{\mathrm{v}}^{w}} - \frac{n_{\mathrm{v}}^{18}\ \mathrm{d}n_{\mathrm{v}}^{w}}{n_{\mathrm{v}}^{w}\ n_{\mathrm{v}}^{w}} \tag{20} $$

$$ = \frac{\mathrm{d}n_{\mathrm{v}}^{18}}{n_{\mathrm{v}}^{w}} - R_{\mathrm{v}}^{18}\frac{\mathrm{d}n_{\mathrm{v}}^{w}}{n_{\mathrm{v}}^{w}} \tag{21} $$

$$ = \frac{\mathrm{d}n_{\mathrm{v}}^{w}}{n_{\mathrm{v}}^{w}}\left(\frac{\mathrm{d}n_{\mathrm{v}}^{18}}{\mathrm{d}n_{\mathrm{v}}^{w}} - R_{\mathrm{v}}^{18}\right) \tag{22} $$

Noting that:

$$ \frac{\mathrm{d}n_{\mathrm{v}}^{18}}{\mathrm{d}n_{\mathrm{v}}^{w}} = R_{\mathrm{c}}^{18} \tag{23} $$

where R_{c}^{18} is the ratio of the condensate removed, it follows:

$$ \mathrm{d}R_{\mathrm{v}}^{18} = \frac{\mathrm{d}n_{\mathrm{v}}^{w}}{n_{\mathrm{v}}^{w}}\left(R_{\mathrm{c}}^{18} - R_{\mathrm{v}}^{18}\right) \tag{24} $$

Since the condensate is formed at equilibrium with the vapor:

$$ R_{\mathrm{c}}^{18} = \alpha_{\text{l-v}}^{18}\ R_{\mathrm{v}}^{18} \tag{25} $$

Thus, replacing this form in the previous equation, it naturally follows that:

$$\mathrm{d}R_\mathrm{v}^{18} = \frac{\mathrm{d}n_\mathrm{v}^w}{n_\mathrm{v}^w} R_\mathrm{v}^{18} \left(\alpha_\text{l-v}^{18} - 1\right) \tag{26}$$

Re-writing the equation in a differential form yield:

$$\frac{\mathrm{d}R_\mathrm{v}^{18}}{R_\mathrm{v}^{18}} = \frac{\mathrm{d}n_\mathrm{v}^w}{n_\mathrm{v}^w} \left(\alpha_\text{l-v}^{18} - 1\right) \tag{27}$$

5 The latter equation may be integrated as follows:

$$\ln\left(R_\mathrm{v}^{18}\right) - \ln\left({}^0R_\mathrm{v}^{18}\right) = \left(\alpha_\text{l-v}^{18} - 1\right)\left(\ln\left(n_\mathrm{v}^w\right) - \ln\left({}^0n_\mathrm{v}^w\right)\right) \tag{28}$$

Using an exponential to simplify the previous form, the traditional form of the Rayleigh distillation is obtained:

$$R_\mathrm{v}^{18} =^0 R_\mathrm{v}^{18} \left(\frac{n_\mathrm{v}^w}{{}^0n_\mathrm{v}^w}\right)^{\alpha_\text{l-v}^{18}-1} \tag{29}$$

10 and using f the remaining fraction of vapor in the moist air mass to simplify the previous form:

$$R_\mathrm{v}^{18} =^0 R_\mathrm{v}^{18}\, f^{\alpha_\text{l-v}^{18}-1} \tag{30}$$

In the following I compare the results for δ^{18}O in precipitation to the results obtained in a theoretical Rayleigh distillation assumed to start from a 0 ‰ as first condensate.

3.1.2 Comparison with model results

Figure 2 shows such a Rayleigh distillation for a constant temperature of 15 °C. Model results (plotted in a color code representing their latitude) are, as expected, largely above the theoretical Rayleigh distillation line. This is expected since the moist air in the model is not isolated at first and thus is recharched over its course from the evaporative regions to the δ^{18}O depleted regions with higher δ^{18}O content from the surface (oceanic mainly). Overall, the evolution of δ^{18}O in precipitation is following the Rayleigh distillation, which shows that the δ^{18}O module computes the ratios in precipitation reasonably.

The points present below the theoretical line are not problematic since there are dry regions with mean temperatures for condensation lower than 15 °C that could be approximated by a colder theoretical Rayleigh distillation line. Moreover, the implementation presented is more complex than a simple distillation and thus does not have to fit exactly one particular theoretical line.

A more problematic part that clearly shows up in the modelling results are the points below -25 ‰ from Antarctica. Contrary to the Rayleigh distillation theoretical curve that show a steady decrease in humidity with decreasing δ^{18}O, our modeling results are showing an increase in humidity with decreasing δ^{18}O. Since those points are coming from Antarctica, it is hard to imagine a likely moisture source with decreasing δ^{18}O content over the continent. Antarctica is probably indeed what is the closest at large scale on Earth from a Rayleigh distillation. Hence, this points to an inconsistency in the modelling setup that is discussed further below.

3.2 Dansgaard relationship

An other well-known feature observed initially by Dansgaard (1964) is the local relationship between δ^{18}O in precipitation and the mean annual temperature at the site. Using essentially high latitude sites (low mean annual temperatures) he found that the relationship was well approximated by the following linear approximation for mean annual

Title Page
Abstract | Introduction
Conclusions | References
Tables | Figures
I◀ | ▶I
◀ | ▶
Back | Close
Full Screen / Esc
Printer-friendly Version
Interactive Discussion

values:

$$\delta^{18}\mathrm{O}_{\mathrm{precip.}} = 0.69\,T_{\mathrm{surf.}} - 13.9 \tag{31}$$

where $T_{\mathrm{surf.}}$ is in °C. He also noted that the relationship was not linear anymore for annual mean temperature above 15 °C. The Dansgaard equation was used extensively for paleotemperature evaluation from δ^{18}O measurements in paleoclimate proxy data. However, it is unlikely to always be stable through time (Werner et al., 2000).

Using available data for δ^{18}O in precipitation from the Global Network for Isotopes in Precipitation (IAEA, 2006), a linear fit on this larger dataset (not shown) can be computed, limiting also the temperature up to 15 °C. It results in a slightly lower slope and intercept obtained with an R^2 value of 0.96. The updated equation is:

$$\delta^{18}\mathrm{O}_{\mathrm{precip.}} = 0.61\,T_{\mathrm{surf.}} - 15.6 \tag{32}$$

Hence, the result is very close to the traditional Dansgaard equation. Using a second-order polynomial fit on all data, the fit can even be better and not limited to low annual mean temperatures. The obtained equation is then:

$$\delta^{18}\mathrm{O}_{\mathrm{precip.}} = -0.0043\,T^2_{\mathrm{surf.}} + 0.5\,T_{\mathrm{surf.}} - 13.11 \tag{33}$$

with an R^2 value of 0.977.

Figure 3 presents our modelling results within this framework. The two previous equations are represented together with a second-order polynomial fit on the modelled δ^{18}O from our simulation with equation:

$$\delta^{18}\mathrm{O}_{\mathrm{precip.}} = -0.0064\,T^2_{\mathrm{surf.}} + 0.39\,T_{\mathrm{surf.}} - 8.56 \tag{34}$$

with an R^2 value of 0.911. At first glance, the two second-order polynomials are quite similar in shape over most of the range of the data, although our results are biased towards heavier δ^{18}O values at identical mean annual temperature. Also, the model results yield flatter relationship for high annual mean temperature. Overall, this indicates that our implementation of δ^{18}O in atmospheric moisture yield too low fractionation from oceanic source moisture towards drier regions, as shown from the lower slope of the fitted polynomial.

Additionally, it is quite obvious that the modelled δ^{18}O values below −35 °C are at odd with all fitted lines. All these datapoints are in Antarctica and highlight a clear issue with the fractionation and advection of water isotopes along the path from the lower latitude. Assuming that a realistic estimation of the modelled "Dansgaard relationship" is given by the fitted second-order polynomial on the modelled values at temperatures higher than −35 °C, it seems that the atmospheric moisture – and hence the δ^{18}O in precipitation – is modified by a source with higher δ^{18}O content. Assuming that these anomalous datapoints are on a mixing line between the fitted polynomial and a source of moisture implies that the contaminating source has an isotopic signal of +5 to +10 ‰. Since there is no such δ^{18}O rich source over Antarctica, it is necessary to conclude that the mixing is only apparent and that the cause is to be found in the numerical advection scheme of ECBilt. Such analysis is reinforced by the already noted bias in humidity over Antarctica at very low δ^{18}O content in precipitation (cf. Fig. 2).

Additional checks performed (not reported here) show that indeed in the case of very low humidity content, the numerical advection scheme is not fully conservative, in isotopes and in water moisture and results in absurd δ^{18}O values in precipitation. Correction of such bias will need relatively thorough analysis of the numerical scheme of ECBilt that is beyond the scope of the present study. It is however noteworthy that the presented implementation of δ^{18}O yield a very positive result by enabling to detect some defects in extremely dry climatic regions, a fact that was ignored so far.

To summarize, we can state that – apart from Antarctica – the relationship modelled between δ^{18}O in precipitation and surface temperature bears a strong ressemblance with what is expected from data inferences, albeit with a lower slope. This lower slope is probably a consequence of the simplicity of the model with the discretisation of atmospheric moisture in a single layer. The fit is also better with a second-order polynomial in the model world than with a linear relationship, as is the case for observations.

3.3 Annual δ^{18}O amplitude

So far, only annual mean values were reported. Since many of the proxy records may have a seasonal bias or record seasonal changes, it is important to have a look at basic features of the seasonal cycle, to verify whether the model is capable of reproducing some aspects of the yearly variations. I choose to present the maximum δ^{18}O amplitude in precipitation from monthly data to evaluate the geographical variations of the amplitude of the seasonal cycle.

The first evident feature from Fig. 4 is the contrast between the continental and the oceanic regions. Over the oceans, the amplitude remains low. Tropical areas are characterised by $\simeq 1$ ‰ amplitude, since the very active evaporation brings moisture in all year round, buffered by the ocean δ^{18}O around 0 ‰. The amplitude increases towards the higher latitudes, but also in the equatorial regions. The maximum amplitude is reached over the Arctic ocean where cold and dry winters, with sea-ice covered ocean yield very low δ^{18}O values and the retreat of sea-ice and influence of warmer sea-surface conditions increases the δ^{18}O during the rest of the year.

Looking at the longitudinal evolution, we see that the amplitude over the continent is several ‰ higher than in the adjacent ocean, an expected result since over the continent there is no buffering effect from a large water body as the ocean. Over Africa for example, the amplitude is comprised between 4 and 9 ‰, while over the neighbouring ocean is between 2 and 4 ‰. Such a result is encouraging and shows that our model capture correctly some expected large-scale patterns of climate and δ^{18}O variations. Again, it shows that the implementation of the water isotopes seems to function correctly in the atmospheric component.

4 Verification: oceanic component

As the focus is on verification of the implementation within the oceanic model and not on validation of the oceanic model itself, I will concentrate on a well-known relationship of the observed ocean: the δ^{18}O–salinity relationship. Since both salinity and δ^{18}O are affected by the balance between evaporation (that extract freshwater from the ocean) and input terms (precipitation, runoff etc. providing freshwater), it is logical that a certain relationship exists between the two terms Craig and Gordon (1965). However, the water extracted by evaporation does not include salt at all (it is pure freshwater) whereas it contains ^{18}O. Thus the relationship is likely to break in hydrologically very active regions that is where the local hydrological balance is dominant over the surface advection and mixing terms. Similarly in the small regions where the sea-ice formation is dominant, the rejection of large amount of salt into the surface oceanic waters with no similar ^{18}O counterpart may alter this relationship.

Figure 5 present results from the simulation for the surface Atlantic data. The distribution within the δ^{18}O–salinity space shows a good correlation between the two variables within the range simulated. Using a linear regression, we obtain a slope of 0.43 to be compared to 0.52 when the same linear regression is performed on modern observations (Schmidt et al., 1999) of the GISS database (not shown). The agreement between the two slopes is excellent, showing our ability to simulate correctly both salinities and δ^{18}O as described in the implementation. The modelled intercept is −14.9 ‰ while the one calculated on data is −17.9. The end-member of the modelling results are thus 3 ‰ too high. Since the δ^{18}O of precipitation is also positively biased around values of −20 ‰ by about 5 ‰ (see Fig. 3), the positive bias toward depleted δ^{18}O values is expected to show also in the oceanic values. The fact that our slope is also underestimated by 0.1 ‰ (δ^{18}O)/ ‰ (salinity) is also related to the same phenomenon.

5 Conclusions

In the present study, I have presented the design, implementation and verification of a δ^{18}O water isotopic module in a simplified, single moisture layer, atmospheric model. The verification step showed that the implementation was successful and that well-known relationships of δ^{18}O with other climatic variables (temperature, humidity) are well represented. I have shown as well that the moisture content was not fully conserved over Antarctica causing unrealistic results for δ^{18}O in precipitation over that region. Since the replacement of the advection module of ECBilt on its Gaussian grid is beyond the scope of the present study, we have analysed the biases that such an non-conservation caused. Though problematic for future use of the isotopic model over Antarctica where some of the most well-known data is recorded in ice-cores (e.g. EPICA community members, 2004), this example is interesting to point out the benefits of water isotope modeling already for the validation of climate models.

The *i*LOVECLIM climate model was developed further with the introduction of an additional scheme to simulate the same δ^{18}O water isotope in the ocean, land-surface and vegetation part of our fully coupled climate model. The analysis of the results from an oceanic perspective showed a good accordance with observation-derived relationships, though still presenting similar biases as the ones detected in the atmospheric part.

Overall, the model seems to perform adequatedly when its simplicity is taken into account. The availability of water isotopes in such a fast model open wide prospects for long-term paleoclimate simulations.

Acknowledgements. D. M. Roche is supported by NWO through the VIDI/AC^{2}ME project no. 864.09.013 and by CNRS-INSU. The author wish to thank A. Landais for useful discussion on isotopic fractionation process, D. Paillard for discussion pertaining to technical developments of the ocean part of the model and T. Caley for comments on a previous version of the manuscript. Institut Pierre Simon Laplace is acknowledged for hosting the *i*LOVECLIM model code under the LUDUS framework project (https://forge.ipsl.jussieu.fr/ludus). All figures except Fig. 1 where produced using the Matplotlib software (Hunter, 2007), whose creators are gratefully acknowledged. This is NWO/AC^{2}ME contribution number 01.

The publication of this article is financed by CNRS-INSU.

References

Berger, A.: Long-term variations of caloric insolation resulting from earths orbital elements, Quaternary Res., 9, 139–167, 1978. 1477

Caley, T. and Roche, D. M.: δ^{18}O water isotope in the *i*LOVECLIM model (version 1.0) – Part 3: A paleoperspective based on present-day data-model comparison for oxygen stable isotopes in carbonates, Geosci. Model Dev. Discuss., 6, 1527–1558, doi:10.5194/gmdd-6-1527-2013, 2013. 1470

Cappa, C. D., Hendricks, M. B., DePaolo, D. J., and Cohen, R. C.: Isotopic fractionation of water during evaporation, J. Geophys. Res., 108, 4525, doi:10.1029/2003JD003597, 2003. 1472, 1473

Craig, H. and Gordon, L.: Deuterium and Oxygen 18 Variations in the Ocean and the Marine Atmosphere, Consiglio Nazionale delle Ricerche, Laboratorio di Geologia Nuclerne, Pisa, 9–130, 1965. 1468, 1469, 1476, 1484

Dansgaard, W.: Stable isotopes in precipitation, Tellus, 16, 436–468, 1964. 1468, 1480, 1492

Dansgaard, W., Johnsen, S., Clausen, H., Dahl-Jensen, D., Gundestrup, N., Hammer, C., Hvidberg, C., Steffensen, J., Sveinbjoernsdottir, A., Jouzel, J., and Bond, G.: Evidence for general instability of climate from a 250-kyr ice-core record, Nature, 364, 218–220, 1993. 1468

Delaygue, G., Jouzel, J., and Dutay, J.-C.: Oxygen 18-salinity relationship simulated by an oceanic general circulation model, Earth Planet. Sc. Lett., 178, 113–123, doi:10.1016/S0012-821X(00)00073-X, 2000. 1469

Emiliani, C.: Pleistocene temperatures, J. Geol., 63, 538–577, 1955. 1468

EPICA community members: Eight glacial cycles from an Antarctic ice core, Nature, 429, 623–628, doi:10.1038/nature02599, 2004. 1468, 1485

Goosse, H., Brovkin, V., Fichefet, T., Haarsma, R., Huybrechts, P., Jongma, J., Mouchet, A., Selten, F., Barriat, P.-Y., Campin, J.-M., Deleersnijder, E., Driesschaert, E., Goelzer, H., Janssens, I., Loutre, M.-F., Morales Maqueda, M. A., Opsteegh, T., Mathieu, P.-P., Munhoven, G., Pettersson, E. J., Renssen, H., Roche, D. M., Schaeffer, M., Tartinville, B., Timmermann, A., and Weber, S. L.: Description of the Earth system model of intermediate complexity LOVECLIM version 1.2, Geosci. Model Dev., 3, 603–633, doi:10.5194/gmd-3-603-2010, 2010. 1470

Hoffmann, G., Werner, M., and Heimann, M.: Water isotope module of the ECHAM atmospheric general circulation model: a study on timescale from days to several years, J. Geophys. Res., 103, 16871–16896, doi:10.1029/98JD00423, 1998. 1469

Hunter, J. D.: Matplotlib: a 2-D graphics environment, Comput. Sci. Eng., 9, 90–95, 2007. 1485

IAEA: Isotope Hydrology Information System, The ISOHIS Database, available at: http://www.iaea.org/water (last access: March 2012) , 2006. 1481

Joussaume, S., Jouzel, J., and Sadourny, R.: A general circulation model of water isotope cycles in the atmosphere, Nature, 311, 24–29, 1984. 1469

Kurita, N., Noone, D., Risi, C., Schmidt, G. A., Yamada, H., and Yoneyama, K.: Intraseasonal isotopic variation associated with the Madden–Julian Oscillation, J. Geophys. Res., 116, D24101, doi:10.1029/2010JD015209, 2011. 1468

Legrande, A. N. and Schmidt, G. A.: Ensemble, water isotope-enabled, coupled general circulation modeling insights into the 8.2 ka event, Paleoceanography, 23, PA3207, doi:10.1029/2008PA001610, 2008. 1469

Majoube, M.: Fractionnement en oxygène 18 entre la glace et la vapeur d'eau, J. Chim. Phys., 68, 625–636, 1971a. 1475

Majoube, M.: Fractionnement en oxygène 18 entre l'eau et sa vapeur, J. Chim. Phys., 68, 1423–1436, 1971b. 1474

Mathieu, R., Pollard, D., Cole, J. E., White, J. W. C., Webb, R. S., and Thompson, S. L.: Simulation of stable water isotope variations by the GENESIS GCM for modern conditions, J. Geophys. Res., 107, 4037, doi:10.1029/2001JD900255, 2002. 1469

Melling, H. and Moore, R. M.: Modification of halocline source waters during freezing on the Beaufort Sea shelf: evidence from oxygen isotopes and dissolved nutrients, Cont. Shelf Res., 15, 89–113, 1995. 1476

Merlivat, L.: The dependence of bulk evaporation coefficients on air–water interfacial conditions as determined by the isotopic method, J. Geophys. Res., 83, 2977–2980, 1978. 1473

Merlivat, L. and Jouzel, J.: Global climatic interpretation of the deuterium-oxygen 18 relationship for precipitation, J. Geophys. Res., 84, 5029–5033, 1979. 1471, 1474

Noone, D. and Simmonds, I.: Associations between delta O-18 of water and climate parameters in a simulation of atmospheric circulation for 1979–95, J. Climate, 15, 3150–3169, doi:10.1175/1520-0442(2002)015<3150:ABOOWA>2.0.CO;2, 2002. 1469

North Greenland Ice Core Project members: High-resolution record of Northern Hemisphere climate extending into the last interglacial period, Nature, 431, 147–151, doi:10.1038/nature02805, 2004. 1468

Opsteegh, J., Haarsma, R., Selten, F., and Kattenberg, A.: ECBILT: a dynamic alternative to mixed boundary conditions in ocean models, Tellus, 50, 348–367 , 1998. 1470

Risi, C., Bony, S., Vimeux, F., Frankenberg, C., Noone, D., and Worden, J.: Understanding the Sahelian water budget through the isotopic composition of water vapor and precipitation, J. Geophys. Res., 115, D24110, doi:10.1029/2010JD014690, 2010a. 1468

Risi, C., Bony, S., Vimeux, F., and Jouzel, J.: Water-stable isotopes in the LMDZ4 general circulation model: model evaluation for present-day and past climates and applications to climatic interpretations of tropical isotopic records, J. Geophys. Res., 115, D12118, doi:10.1029/2009JD013255, 2010b. 1469

Roche, D. M. and Caley, T.: δ^{18}O water isotope in the *i*LOVECLIM model (version 1.0) – Part 2: Evaluation of model results against observed δ^{18}O in water samples, Geosci. Model Dev. Discuss., 6, 1495–1525, doi:10.5194/gmdd-6-1495-2013, 2013. 1470

Roche, D., Paillard, D., and Cortijo, E.: Constraints on the duration and freshwater release of Heinrich event 4 through isotope modelling, Nature, 432, 379–382, 2004. 1469

Schmidt, G. A.: Oxygen-18 variations in a global ocean model, Geophys. Res. Lett., 25, 1201–1204, doi:10.1029/98GL50866, 1998. 1469

Schmidt, G. A., Bigg, G. R., and Rohling, E. J.: Global Seawater Oxygen-18 Database – V1.21, available at: http://www.giss.nasa.gov/data/o18data/ (last access: March 2012) , 1999. 1484

Tindall, J. C., Valdes, P. J., and Sime, L. C.: Stable water isotopes in HadCM3: isotopic signature of El Nino Southern Oscillation and the tropical amount effect, J. Geophys. Res., 114, D04111, doi:10.1029/2008JD010825, 2009. 1469

Werner, M., Mikolajewicz, U., Heimann, M., and Hoffmann, G.: Borehole versus isotope temperatures on Greenland: seasonnality does matter, Geophys. Res. Lett., 27, 723–726, 2000. 1481

Werner, M., Langebroek, P. M., Carlsen, T., Herold, M., and Lohmann, G.: Stable water isotopes in the ECHAM5 general circulation model: toward high-resolution isotope modeling on a global scale, J. Geophys. Res.-Atmos., 116, D15109, doi:10.1029/2011JD015681, 2011. 1469

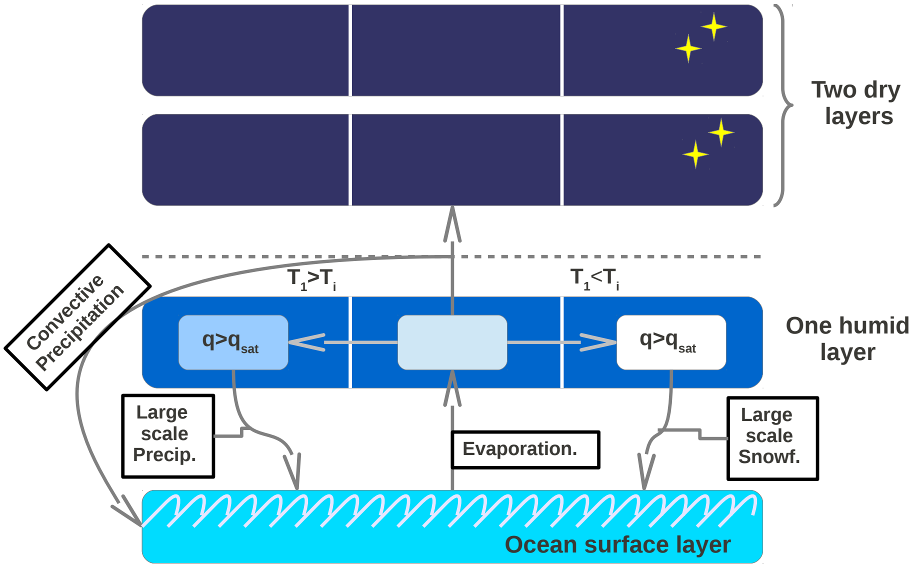

Fig. 1. Schematic representation of the water cycle in ECBilt. The abbreviation are as follow: q_{sat} stands for saturation humidity and q for humidity; T_i stands for limit temperature for snowfall and T_1 is the temperature of the first layer of the atmosphere; "Snowf." stands for Snowfall and "Precip" for precipitation.

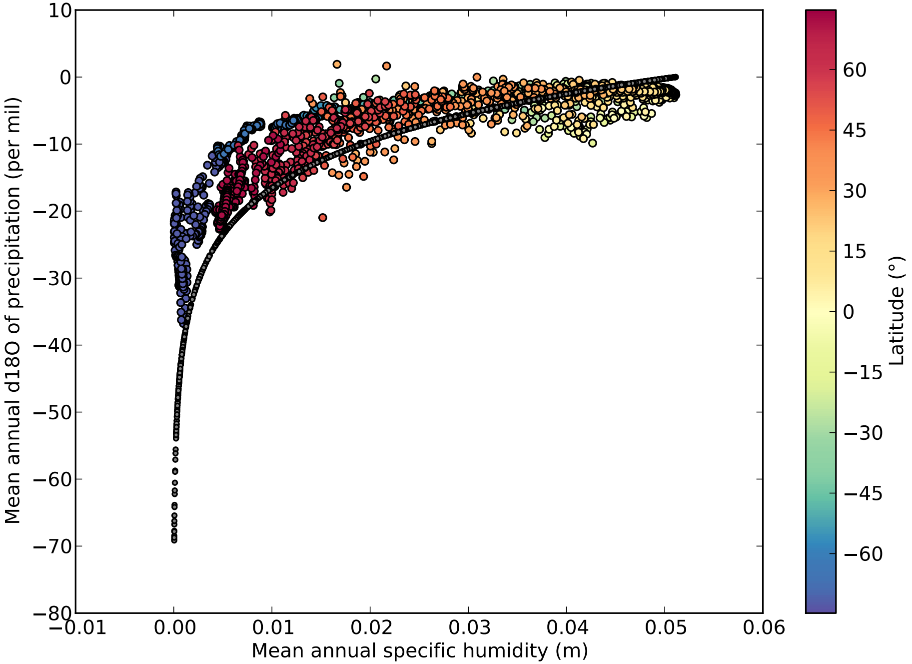

Fig. 2. δ^{18}O–humidity relationship in *i*LOVECLIM compared to a theoretical Rayleigh distillation model. The colorscale applied to model points indicates the latitude. The Rayleigh distillation curve is given for a temperature of 15 °C starting from an oceanic-like value of 0 ‰, as an example.

Title Page
Abstract
Introduction
Conclusions
References
Tables
Figures
◀▌
▶▌
◀
▶
Back
Close
Full Screen / Esc
Printer-friendly Version
Interactive Discussion

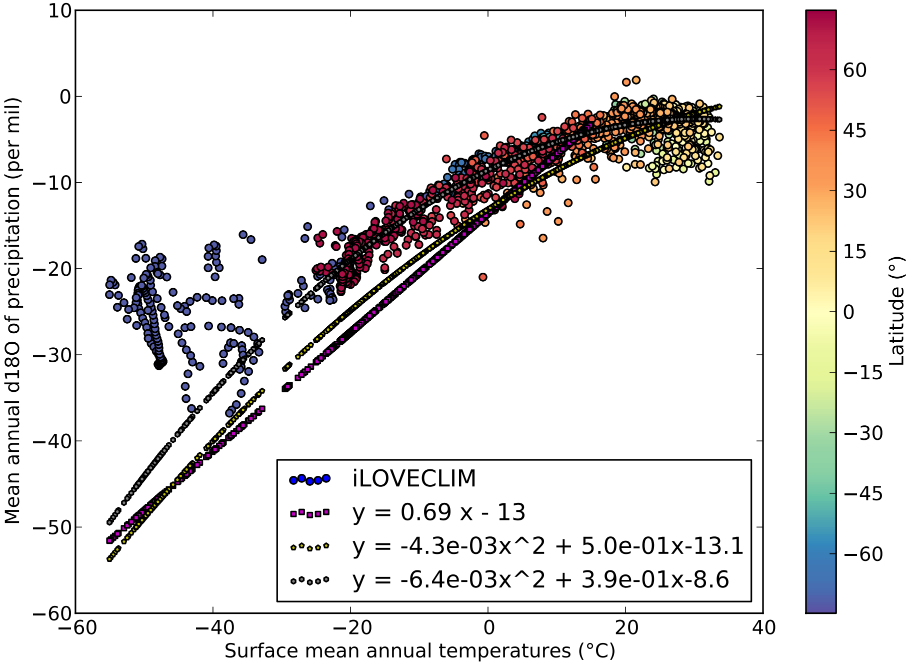

Fig. 3. Annual δ^{18}O–temperature relationship in *i*LOVECLIM compared to the original regression from Dansgaard (1964). Colored dots are from the model simulation, colored after their latitude, given on the scale to the right; grey dots is the fitted second-order polynomial to the model data for temperature above −30 °C; magenta dots are constructed from the temperature data in *i*LOVECLIM, using the regression from Dansgaard (1964); yellow dots are constructed from the temperature data in *i*LOVECLIM using a second order polynomial fitted to te GNIP dataset. R^2 values for the fit to the *i*LOVECLIM model is 0.911 (grey dots); R^2 values for the fit to the GNIP data is 0.977 (yellow dots).

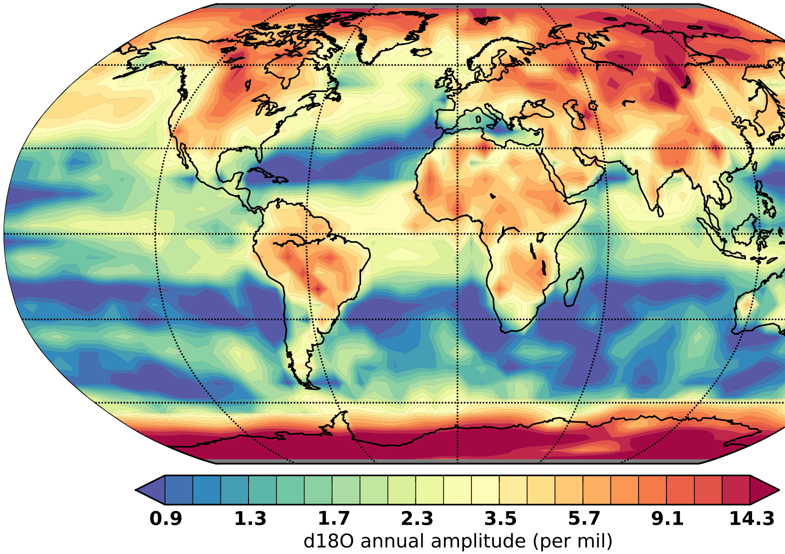

Fig. 4. Annual $\delta^{18}O$ amplitude in precipitation in *i*LOVECLIM computed from monthly mean climatology. The amplitude is calculated as: $\Delta\delta^{18}O = \text{maximum}(\delta^{18}O(m), m) - \text{minimum}(\delta^{18}O(m), m)$; $m = 1, 12$ where m stands for the months of the year.

Title Page

Abstract | Introduction

Conclusions | References

Tables | Figures

◀❙ | ❙▶

◀ | ▶

Back | Close

Full Screen / Esc

Printer-friendly Version

Interactive Discussion

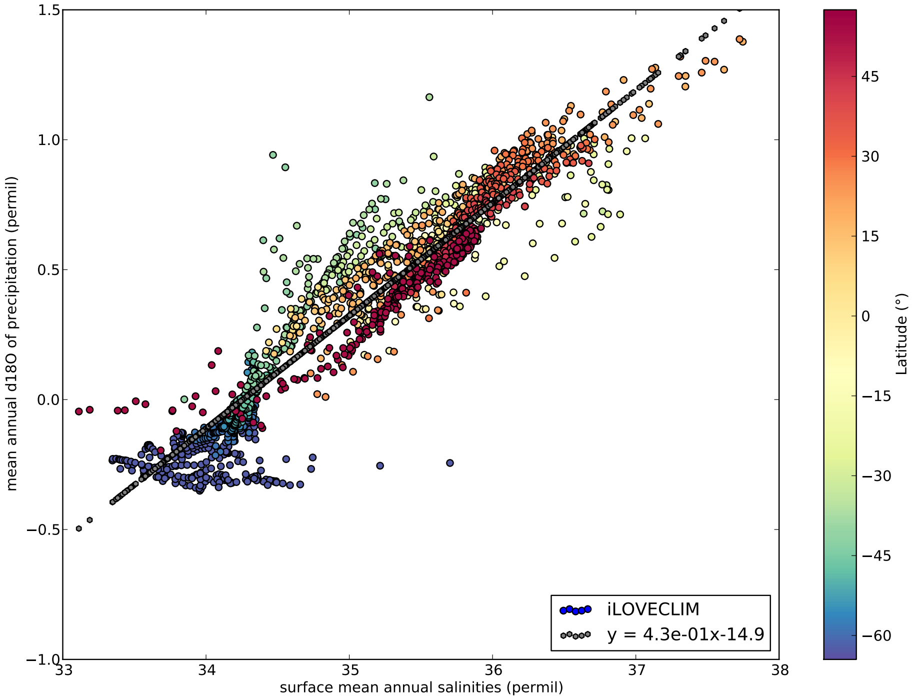

Fig. 5. Near surface ocean annual δ^{18}O–salinity relationship in *i*LOVECLIM for the Atlantic Ocean. Linear fit to the model data is given in the equation in the bottom right box, with a R^2 coefficient of 0.877. Performing the same analysis on Atlantic Ocean data from the GISS database, we obtain a linear regression of $0.52\,x - 17.9$ with a R^2 of 0.81. The colorscale applied on modelled points is the given latitude of each point.